Journal of the European Ceramic Society **12** (1993) 79–86

Mixed Electronic/Ionic Conductivity of the Solid Solution $La_{(1-x)}Sr_xCo_{(1-y)}Ni_yO_{3-\delta}$ (x: 0·4, 0·5, 0·6 and y: 0·2, 0·4, 0·6)

Ch. Ftikos

Laboratory of Inorganic Materials Technology, Department of Chemical Engineering, NTU of Athens, 9 Iroon Polytechniou Str., Zografou Campus, Athens 15780, Greece

S. Carter & B. C. H. Steele

Centre of Technical Ceramics, Department of Materials, Imperial College, Prince Consort Road, London SW7 2BP, UK

(Received 30 October 1992; revised version received 10 February 1993; accepted 12 February 1993)

Abstract

The effect of Sr and Ni substitution on the mixed electronic/ionic conductivity was investigated in a series of the perovskite-type oxides $La_{(1-x)}Sr_xCo_{(1-y)}Ni_yO_{3-\delta}$ *(x: 0·4, 0·5, 0·6 and y: 0·2, 0·4, 0·6) prepared. Electrical conductivity was measured, in air, by a four-point probe technique, within the temperature range 500–1000°C. Oxygen self-diffusion coefficient (D*), activation energy* (E_a)*, and surface exchange (k) data were obtained, by combining the isotopic* $^{18}O/^{16}O$ *exchange diffusion profile (IEDP) technique, at 700, 800 and 900°C, with the secondary ion mass spectroscopy (SIMS) technique for the* ^{18}O *depth profile measurement.*

The results derived suggest that the present perovskite-type oxides are excellent mixed conductors, having high electronic conductivity in addition to their high O^{2-} *self-diffusivity. Oxygen flux through the material was principally controlled by the surface exchange kinetics. As far as the effect of Sr and Ni substitution on the electrical properties is concerned, a strong interdependence was found between the dopant's content.*

Der Effekt der Sr- und Ni-Substitution auf die gemischte elektronische/ionische Leitfähigkeit wurde in einer Reihe von perowskitischen ($La_{(1-x)}Sr_xCo_{(1-y)}Ni_yO_{3-\delta}$*) Oxiden der Zusammensetzung (x: 0·4, 0·5, 0·6 und y: 0·2, 0·4, 0·6) untersucht. Die elektrische Leitfähigkeit wurde mit Hilfe einer Vier-Punkt-Methode in Luft im Temperaturbereich von 500 bis 1000°C gemessen. Daten bezüglich der Sauerstoffselbstdiffusion (D*), der Aktivierungsenergie* (E_a) *und Grenzflächenaustausch (k) wurden mit einer kombinierten 'Isotope* $^{18}O/^{16}O$ *Exchange Diffusion Profile' (IEDP) Techyik bei 700, 800 und 900°C und Sekundär-Ionen Massen Spektrometrie (SIMS) Technik für die* ^{18}O *Tiefenprofilmessungen bestimmt.*

Die erhaltenen Ergebnisse zeigen, daß die untersuchten Oxide vom Perowskit-Typ ausgezeichnete Mischleiter mit hoher elektronischer Leitfähigkeit zusätzlich zu ihrer hohen O^{2-} *Selbstdiffusion sind. Der Sauerstoff fluß durch das Material wird durch die Grenzflächenaustauschkinetik kontrolliert. Die elektrischen Eigenschaften hängen vom Sr- und Ni- Gehalt mit starker gegenseitiger Beeinflussung ab.*

L'effet de la substitution avec Sr et Ni dans une série d'oxides de type perovskite $La_{(1-x)}Sr_xCo_{(1-y)}Ni_yO_{3-\delta}$ *(x: 0·4, 0·5, 0·6 and y: 0·2, 0·4, 0·6) sur la conductivité mixte électronique/ionique a été étudié. La conductivité électrique a été mésurée dans l'air entre 500 et 1000°C par la méthode des quatre points. Le coefficient d'auto-diffusion (D*), l'énergie d'activation* (E_a) *et le coefficient d'échange en surface (k) ont été obtenus en effectuant des échanges d'isotopes d'oxygène (*$^{18}O/^{16}O$*) (IEDP) à 700, 800 et 900°C et en mesurant le profil en profondeur de* ^{18}O *par (SIMS).*

Les résultats obtenus suggèrent que ces oxydes de type perovskite, ayant une conductivité électronique et un coefficient d'autodiffusion élevés, sont des excellents conducteurs mixtes. Le flux d'oxygène à travers le matériau est contrôlé principalement par la

Journal of the European Ceramic Society 0955-2219/93/$6.00

cinétique d'échange en surface. En ce qui concerne l'effet de la substitution avec Sr et Ni sur les propriétés électriques, une forte dépendance réciproque entre les contenus des deux éléments dopants a été remarquée.

1 Introduction

So far mixed conduction has been reported for many oxide systems, such as Bi_2O_3–$Tb_2O_{3.5}$,[1] $BaY_2Cu_3O_{7-x}$,[2,3] $Ba_3In_2ZrO_8$,[4] ZrO_2–CeO_2–Y_2O_3,[5] etc. Perovskite-type oxides (ABO_3) have been the subject of many crystallographic, magnetic and conductivity investigations. It has been pointed out that various functional properties of these nonstoichiometric oxides can easily be modified by total or partial substitution of cations at A and/or B sites. Such a typical property is the mixed conductivity presented by both oxide ions and electronic charge carriers (electrons or holes). Technological applications include dense ceramic membranes[6-12] and cathodes for high-temperature fuel cells.[13-19]

The defect chemistry of the doped $LaCoO_3$ composition is complicated by the fact that the predominant defect region in the relevant Brouwer diagram will be a function of the temperature, oxygen partial pressure and the redox stability of the appropriate transition metal cation. An approach to the overall situation has been summarised by Steele.[15]

Furthermore, it has already been reported that the solid oxide system $La_{0.6}A_{0.4}Co_{0.8}B_{0.2}O_{3-\delta}$ (A: Sr, Ca and B: Fe, Co, Ni, Cu, Mn) exhibits high ionic conductivities (10^{-2}–10^{0} S/cm at 1073 K) in addition to high electronic conductivity (10^{2}–10^{3} S/cm). It is also reported that the oxygen permeability is roughly proportional to the oxide ion conductivities.[16,17,20-22]

Thus, in an extensive research program, attempts have been focused on the investigation and optimisation of the properties of these ceramics. In a recent paper[23] the influence of Sr and Ni substitution in $LaCoO_3$ on the stability of the phases formed and their thermal properties have been examined. In the present paper the effect of these elements on the electronic conductivity and oxygen self-diffusion is studied.

2 Experimental

2.1 Sample preparation

Four series of perovskite-type oxides were prepared as shown in Table 1. The starting materials used were the acetate salts of La, Sr, Co and Ni, respectively and citric acid, all of analytical grade. Each of the reagents was dissolved in distilled water and the concentration of the ions was measured using the atomic absorption spectroscopy (AAS) technique. A solution then was formed by taking the required proportion of the ions and citric acid added in order to bind all the metal ions. By maintaining the solution in a hot plate, a gel of the citrates of the metals was formed, giving upon decomposition a fine homogenous powder, which calcined at 1000°C

Table 1. Composition, lattice parameters and crystal structure of the oxides prepared

Code	*Composition*[a]	*Lattice parameter*		*Crystal structure*
		a (Å)	*c* (Å)	
Series 0				
A_0	$La_{0.6}Sr_{0.4}CoO_{2.80}$	3.840(1)	—	Cubic
D_0	$La_{0.8}Sr_{0.2}CoO_{2.9}$	3.849(2)	—	Cubic
D_1	$La_{0.8}Sr_{0.2}Co_{0.8}Ni_{0.2}O_{2.8}$	3.844(3)	—	Cubic
Series 1				
A_1	$La_{0.6}Sr_{0.4}Co_{0.8}Ni_{0.2}O_{2.70}$	3.835(1)	—	Cubic
B_1	$La_{0.5}Sr_{0.5}Co_{0.8}Ni_{0.2}O_{2.65}$	3.828(1)	—	Cubic
C_1	$La_{0.4}Sr_{0.6}Co_{0.8}Ni_{0.2}O_{2.60}$	3.827(1)	—	Cubic
Series 2[b]				
A_2	$La_{0.6}Sr_{0.4}Co_{0.6}Ni_{0.4}O_{2.60}$	3.827(1)	—	Cubic
		3.805(2)	12.443(8)	Tetragonal
B_2	$La_{0.5}Sr_{0.5}Co_{0.6}Ni_{0.4}O_{2.55}$	3.820(2)	—	Cubic
		3.805(3)	12.422(9)	Tetragonal
C_2	$La_{0.4}Sr_{0.6}Co_{0.6}Ni_{0.4}O_{2.50}$	3.839(2)	—	Cubic
		3.811(1)	12.473(6)	Tetragonal
Series 3				
A_3	$La_{0.6}Sr_{0.4}Co_{0.4}Ni_{0.6}O_{2.50}$	3.813(1)	12.503(2)	Tetragonal
B_3	$La_{0.5}Sr_{0.5}Co_{0.4}Ni_{0.6}O_{2.45}$	3.811(1)	12.505(2)	Tetragonal
C_3	$La_{0.4}Sr_{0.6}Co_{0.4}Ni_{0.6}O_{2.40}$	3.811(1)	12.509(5)	Tetragonal

[a] The oxygen stoichiometry has been calculated assuming the following valences: La^{3+}, Sr^{2+}, Co^{3+}, Ni^{2+}.
[b] Two phases are observed.

for 10 h. The powders were pressed into pellets under a uniaxial compaction of 300 MPa and sintered in air at 1250°C for 10 h. Heating and cooling rate was 5°C/min.

The bulk density of all the specimens was measured and found to be more than 92% of the theoretical density. Also, the specimens were analysed by means of the SEM–EDAX technique, particularly in respect of La, Sr, Co and Ni contained, and the compositions of the phases presented in Table 1 was confirmed.

2.2 Electrical conductivity measurements

The electrical conductivity was monitored in the temperature range 500 to 1000°C, using the four-point probe DC technique. Four platinum (Pt) wire contacts were made to the pellets (two at each side) as follows. Both sides of the sample were covered with Pt paste. Then Pt gauze was embedded in them, since the Pt wire had been initially fitted in the gauze. The system was fired at 1000°C in order to stabilise the Pt electrodes. Two connections (one at each side of the pellet) were used to apply the standard current (I) along the length (L) of the two sides and the other two connections were used for measuring the voltage difference (ΔV) between them.

A sample holder, providing the necessary Pt wire connections to the conductivity ring, was used to heat the sample in an horizontal tube furnace. ΔV was recorded after the sample was left at each specific temperature for thirty minutes. The total conductivity (σ_t) was calculated according to the equation:

$$\sigma_t = (I/\Delta V)(L/A)$$

where A is the cross-sectional area of the pellet.

2.3 Oxygen self-diffusion measurements

The isotopic $^{18}O/^{16}O$ exchange diffusion profile (IEDP) technique was used to obtain the diffusion surface exchange data. Small pieces of the sample (about 0·5 cm^2 and 2 mm thick) were polished to 0·25 μm using a diamond spray and cleaned. In order to equilibrate the composition of the specimens prior to ^{18}O exchange, the samples were pre-annealed at the same temperature as that required for the ^{18}O exchange in an atmosphere of dry ^{16}O at a nominal pressure of 0·7 atm. The pre-anneal time was longer than the selected time for the ^{18}O exchange. The ^{18}O exchange was carried out at a selected temperature and for a selected time, in an atmosphere enriched in ^{18}O (70% $^{18}O_2$, 5% $^{16}O_2$ and 25% N_2) at a nominal pressure of 1 atm.

Secondary ion mass spectroscopy (SIMS) was used to obtain the ^{18}O depth distribution profile, using a Xe^+ beam at 10 keV and the line scanning technique[24] for fast diffusers. The values of D^* and k were calculated by fitting the experimental data of the $^{18}O/(^{16}O + ^{18}O)$ depth profiles to the following diffusion equation:[5]

$$\frac{C_x - C_{bg}}{C_g - C_{bg}} = \operatorname{erfc}\left[\frac{x}{2\sqrt{D^*t}}\right] - [\exp(hx + h^2D^*t)]\operatorname{erfc}\left[\frac{x}{2\sqrt{D^*t}} + h\sqrt{D^*t}\right]$$

where C_x = isotopic concentration at depth x,
C_g = isotopic concentration of the gas,
C_{bg} = natural isotopic background,
D^* = self-diffusion coefficient,
k = surface exchange coefficient,
$h = k/D^*$,
t = diffusion time.

3. Results and Discussion

The compositions of the specimens prepared and the structures of the phases formed are shown in Table 1. They have been classified into four series with respect to Sr and Ni subsitution, as well as the crystal structure.

3.1 Electronic conductivity

For a mixed conductor, the electrical conductivity obtained by a standard four-point DC technique refers to the sum of ionic and electronic conductivity. However, in the present solid oxide solutions, the electrical conductivity measured can be regarded as the electronic conductivity within an experimental error, since the electronic conductivity is higher by at least two orders of magnitude than the ionic.

Figure 1 shows the temperature dependence of electronic conductivity (σ_e), measured in air, within the range of 500–1000°C, for the four series of the samples prepared. For all the compositions $La_{(1-x)}Sr_xCo_{(1-y)}Ni_yO_{3-\delta}$ examined, the σ_e was high, ranging from 10^2 to 10^3 S/cm. The magnitude and the negative temperature coefficient of σ_e, in most cases, suggest a metallic-type conductivity within this temperature range. Such metallic-type conduction involves the transition metals. $LaCoO_3$ has $\sigma_e = 1$ S/cm even at room temperature, and metallic conductivity is also reported for $La_{0.6}A'_{0.4}Co_{0.8}B'_{0.2}O_{3-\delta}$ (A': La, Sr, Ca and B': Co, Fe, Cu, Ni).[7,11,25]

Figure 2 presents the electronic conductivity (σ_e) as a function of the values of x, for the various y investigated, at 800°C. Looking at Figs 1 and 2, as well as the values of σ_e at room temperature, presented in Table 2, the following observations are suggested, in respect of the Sr and Ni substitution effect.

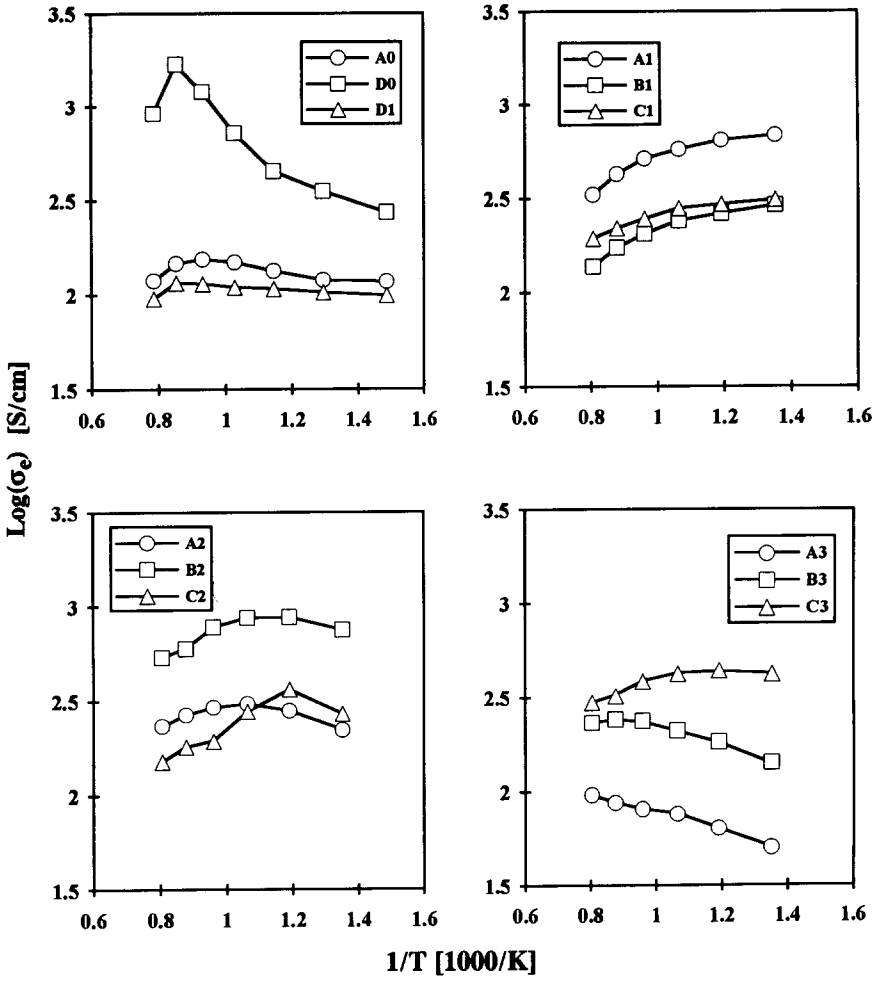

Fig. 1. Electronic conductivity (σ_e) versus reciprocal temperature of the four series of the oxides prepared $La_{(1-x)}Sr_xCo_{(1-y)}Ni_yO_{3-\delta}$.

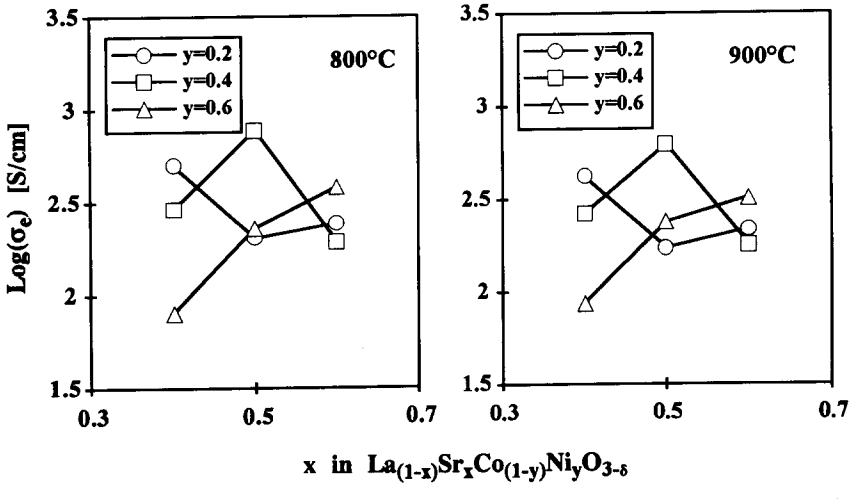

Fig. 2. Electronic conductivity (σ_e) versus the various x and y examined for the oxides $La_{(1-x)}Sr_xCo_{(1-y)}Ni_yO_{3-\delta}$ at 800 and 900°C.

Table 2. Electronic conductivity (σ_e) at room temperature of the oxides prepared

	Sample											
	A_0	D_0	D_1	A_1	B_1	C_1	A_2	B_2	C_2	A_3	B_3	C_3
Log σ_e	2·00	1·98	1·62	2·80	2·73	2·47	1·38	1·30	1·05	0·35	0·68	1·78

Series 0—A_0: $La_{0.6}Sr_{0.4}CoO_{2.8}$; D_0: $La_{0.8}Sr_{0.2}CoO_{2.9}$; D_1: $La_{0.8}Sr_{0.2}Co_{0.8}Ni_{0.2}O_{2.8}$

In sample D_0, σ_e is high and increases with temperature, presenting a usual semiconductive behaviour. Two transitions are observed, the first at 600°C towards higher activation energy (E_a) and the second to metallic conduction at 900°C, which is attributed to the localised collective electron transition.[20-23,26-28] By increasing the Sr content (A_0), the σ_e decreases; however, the material still behaves in a similar way to D_0, with much lower E_a.

In the case of the Ni substitution for Co (D_1), σ_e is also lower than that of D_0 and comparable to A_0. The material has almost a metallic-type conductivity with an E_a near to zero. There is still the transition at 900°C.

Series 1—$La_{1-x}Sr_xCo_{0.8}Ni_{0.2}O_{3-\delta}$, x: 0·4(A_1), 0·5(B_1), 0·6(C_1)

Starting from room temperature, all the compositions present metallic-type conductivity. In sample A_1, σ_e is higher than that of the specimens B_1 and C_1, the last having comparable σ_e. At room temperature, σ_e is also reduced by increasing Sr content.

Series 2—$La_{1-x}Sr_xCo_{0.6}Ni_{0.4}O_{3-\delta}$, x: 0·4(A_2), 0·5(B_2), 0·6(C_2)

In all the cases, the material still behaves with metallic-type conduction. By increasing the Sr content, σ_e decreases at room temperature. Also, this is lower than the σ_e of the samples A_1, B_1 and C_1, being comparable to them at the higher temperature region. The specimen B_2 presents higher σ_e than that of A_2 and B_2, which have almost similar σ_e.

Series 3—$La_{1-x}Sr_xCo_{0.4}Ni_{0.6}O_{3-\delta}$, x: 0·4(A_3), 0·5(B_3), 0·6(C_3)

The compositions A_3 and B_3 present a semiconductor-type conductivity with nearly the same E_a. At room temperature, their conductivity is one order of magnitude lower than that of C_3. In contrast, sample C_3 still behaves as a metallic conductor.

As far as the electronic conductivity is concerned, these observations suggest that there is a strong inter-relationship between Sr and Ni substitutions for La and Co respectively, in the oxides $La_{(1-x)}Sr_xCo_{(1-y)}Ni_yO_{3-\delta}$. A similar dependence has also been suggested in a recent paper for the structure that the phases form.[23] This is attributed to the contribution of Sr, bringing Co^{3+} to the high spin state, but also, it contributes to the oxidation of Ni^{2+} to Ni^{3+} that mainly occurs in perovskites at the low spin state.[25-33]

However, in spite of the two phases presented when the Ni content is more than 20%, the results show that all the present perovskite-type oxides are excellent electronic conductors having a σ_e ranging from 10^2 to 10^3 S/cm. Furthermore, an optimum Ni content at each Sr substitution is suggested for the present oxides, in order to achieve the highest electronic conductivity. Thus, in the case of 40 mol% substitution of Sr for La, the optimum Ni doping for Co is suggested to be 20 mol%, and when the Sr content is 50 mol%, Ni substitution should be 40 mol%.

3.2 Oxygen self-diffusion

The oxygen self-diffusion coefficient (D^*) values of the prepared oxides $La_{(1-x)}Sr_xCo_{(1-y)}Ni_yO_{3-\delta}$ (x: 0·4, 0·5, 0·6 and y: 0·2, 0·4, 0·6) measured in air at the temperatures of 700, 800 and 900°C, are given in Table 3. These are also presented as a function of the

Table 3. Oxygen diffusion data (D^*, E_a, k and h) of the oxides $La_{(1-x)}Sr_xCo_{(1-y)}Ni_yO_{3-\delta}$ (x: 0·4, 0·5, 0·6 and y: 0·2, 0·4, 0·6)

	Sample								
	A_1	B_1	C_1	A_2	B_2	C_2	A_3	B_3	C_3
Oxygen self-diffusion coefficient, D^* (cm^2/s) $\times 10^{-7}$									
At 900°C	4	40	—	3	10	10	6	0·2	0·6
At 800°C	1	20	3	0·6	3	1	0·7	0·2	0·1
At 700°C	0·3	3	1	0·02	0·4	0·5	0·1	0·05	0·05
Activation energy, E_a (kJ/mol)	122±2	125±26	—	255±35	157±10	150±35	187±16	78±21	116±26
Surface exchange coefficient, k (cm/s) $\times 10^{-6}$									
At 900°C	2	7	—	3	8	10	2	1	2
At 800°C	2	8	4	0·3	7	4	2	4	2
At 700°C	2	4	2	0·7	1	4	0·3	0·4	0·5
Oxygen flux balance, $h = D^*/k$ (cm^{-1})									
At 900°C	5	2	—	10	8	10	3	50	33
At 800°C	20	4	13	5	23	40	29	200	200
At 700°C	67	13	20	350	25	80	30	80	100

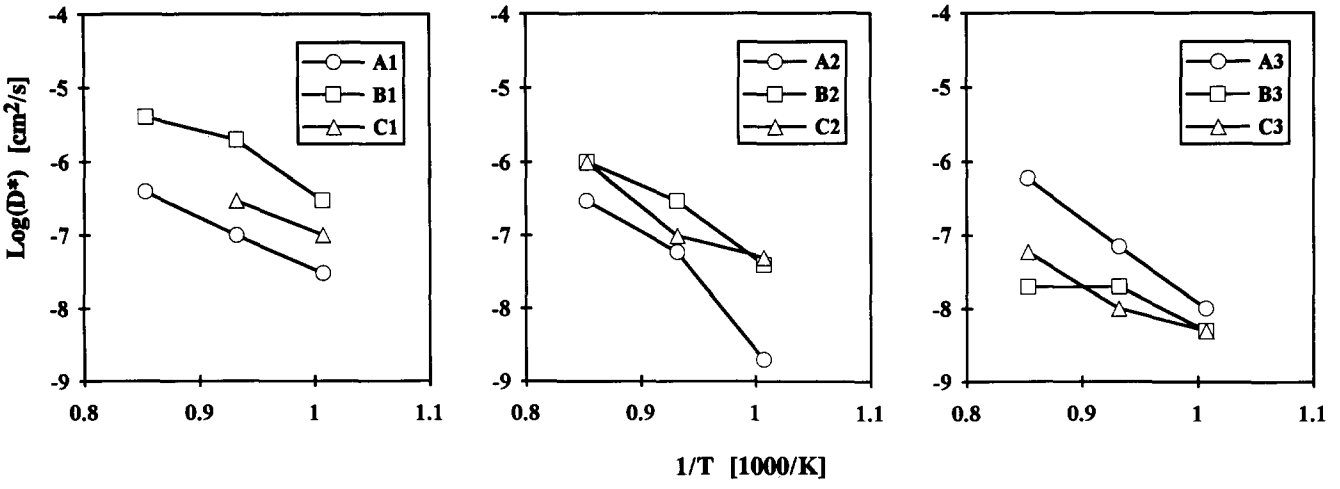

Fig. 3. Oxygen self-diffusion coefficient (D^*) versus reciprocal temperature in the oxides $La_{(1-x)}Sr_xCo_{(1-y)}Ni_yO_{3-\delta}$ (x: 0·4, 0·5, 0·6 and y: 0·2, 0·4, 0·6).

reciprocal temperature in Fig. 3. The D^* value of the sample C_1 (x: 0·4, y: 0·2) has not been measured at 900°C because the sample disintegrated during annealing. The experimental procedure involved rapid heating and cooling cycles which could not be tolerated by the high thermal expansion of the material. For all the compositions the oxygen self-diffusion coefficient D^* was high, ranging from 10^{-6} to 10^{-8} cm^2/s within the temperature range examined.

It is not appropriate to compare the mass transport of all the samples at the same time because of different structures and the presence of two phases (series A_2, B_2, C_2). It is useful, however, to examine the diffusion trends within each series.

In series 1, as the Sr content was increased from 0·4 to 0·5 the oxygen diffusion coefficient increased, but then decreased as the Sr content was increased further (0·6), as shown in Fig. 4. This is a different behaviour than that reported for the series of the compositions $La_{1-x}Sr_xCo_{0.5}Fe_{0.2}O_{3-\delta}$ by Teraoka *et al.*[17] As mentioned earlier, the additions of Sr can

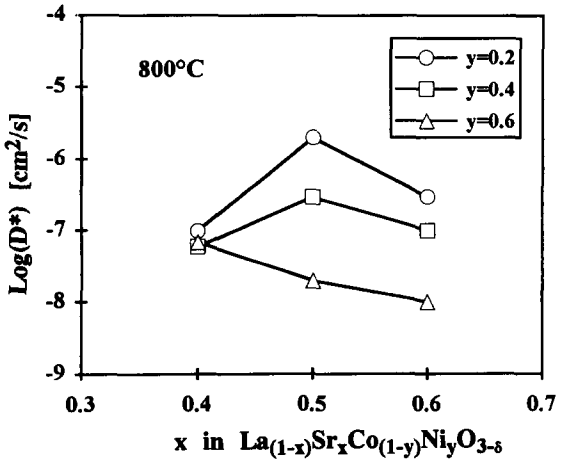

Fig. 4. Oxygen self-diffusion coefficient (D^*) versus the x and y examined in the oxides $La_{(1-x)}Sr_xCo_{(1-y)}Ni_yO_{3-\delta}$ (x: 0·4, 0·5, 0·6 and y: 0·2, 0·4, 0·6) at 800°C.

be compensated by the formation of Co^{4+} or anion vacancies and so, it is important to have further information about the oxygen stoichiometry before meaningful interpretations can be made. The situation is further complicated by the fact that if Sr additions are indeed creating anion vacancies, their mass transport could be reduced by vacancy–vacancy interactions and other complicated defect complexes.

The activation energy measured for diffusion in the composition $La_{0.5}Sr_{0.5}Co_{0.8}Ni_{0.2}O_{3-\delta}$ (B_1) was 125 kJ/mol (29 kcal/mol) which is somewhat higher than the value (23 kcal/mol) reported by Teraoka *et al.*[17] for a similar composition. It is instructive to calculate the oxygen ion conductivity (σ_i) for this composition using the Nernst–Einstein relationship:

$$\sigma_i/D^* = N_i q_i^2/kT \quad \text{at } 1000\,\text{K}$$

The exact stoichiometry of this composition is not known but a value of $O_{2.6}$ ($\delta = 0.4$) was assumed for the calculation and a value of 2.23×10^{-1} S/cm was obtained which compares with a value of 1 S/cm reported by Teraoka *et al.*[17]

The presence of two phases in series 2 makes interpretation even more difficult and no further comments are made on these compositions. With regard to series 3 (tetragonal structure) the highest diffusion was reported for the lowest Sr content at the higher temperatures, but all the compositions exhibited similar diffusion coefficient values at lower temperatures.

Furthermore, the difference in the D^* values of the prepared cobaltites, in respect of the Sr and Ni substitution for La and Co respectively, could be explained by the valence and bond theory. Thus, with increasing doping of Sr for La more vacancies are created and the cobalt is mainly presented in the high spin state (hs). Also, there is a demand for electrical balance, which is equilibrated by transition of some of the Co^{3+} (hs) to Co^{4+}.[20,27] The greater

the Sr content the more O^{2-} vacancies and Co^{3+} (hs) there are, but, in turn, the demand for electrical balance is more intensive. In the case of partial substitution of Ni for Co, suggested to increase vacancies, this intensive demand is alleviated by transformation of more Ni^{2+} to Ni^{3+}, which mainly exists at the low spin state (ls) in the perovskite-type oxides. The increase in Ni^{2+} content results in higher Ni^{3+} (ls) concentrations. The octahedral site low spin Ni^{3+} ($t_{2g}^6 e_g^1$) interacts covalently with the oxygen $2p$ orbital to give an e_g band that is $\frac{1}{4}$ filled.[30] Substitution of nickel for trivalent cobalt would increase the covalent interaction because, as stated above, Co^{3+} occurs mostly in the high spin state and it is known that high spin ions interact less covalently than the corresponding low spin ions.[27] Consequently, Ni^{3+} (ls) formed traps the O^{2-} vacancies and D^* is reduced. This agrees with the model suggested by Steele.[15] For the high Sr and Ni doped cobaltites, the interaction of Ni^{3+} (ls) with O^{2-} would shift the position of the isotherm to the left, compared to the pure cobalitites, thus decreasing the nonstoichiometry of these oxides. This, in turn, would be accompanied by an appropriate decrease in the concentration of oxygen vacancies (V_O).

3.3 Activation energy (E_a) of oxygen self-diffusion

The values of E_a, with the standard errors, obtained from Fig. 3 are given in Table 3. E_a consists of two terms, the enthalpy of migration (ΔH_m) and the association enthalpy (ΔH_a). The first is due to the migration of an oxygen ion through the lattice and is more dependent on the lattice structure than on the dopant cation. The second results from the formation of complex defects such as $[M'_{La}-V_O\cdot\cdot]$·[34–36] and it is strongly dependent upon the dopant cation size. There is an indication that the minimum ΔH_a occurs when the radii of dopant and host cations are about the same.[34] For dilute solid solutions, E_a decreases by decreasing the dopant concentration due to a decrease in ΔH_a.

Most of the compositions prepared exhibit activation energies of 120–150 kJ/mol. There are two extreme cases, samples A_2 and B_3, presenting the lowest and the highest E_a, 80 and 255 kJ/mol, respectively. These values are a little higher than those reported for similar types of compositions (E_a 88–122 kJ/mol) by Teraoka *et al.*[17]

3.4 Surface exchange coefficient (k)

For technological applications the knowledge of surface exchange kinetics is of particular importance, as far as the choice of the solid oxide ion conductor is concerned. k is often the limiting factor for many materials in maintaining the high oxygen fluxes needed. Steele[15] has collated requirements for D^* and k in such applications. Whilst materials of specified D^* are available they do not possess the required k. In this case, oxygen transport across the gas–solid interface is slower than within the material and the total oxygen flux through the mixed conductor is inhibited by the surface exchange kinetics. The k values for the oxides examined are shown in Table 3, ranging from 10^{-6} to 10^{-7} cm/s. The oxygen flux through the material is determined by the balance of the bulk diffusion to the surface exchange rates ($h = k/D^*$). The h values, listed in Table 3, are mostly within the range 2–50 cm^{-1}. The lowest h value was detected for specimen B_1. The samples A_2, B_3 and C_3 present higher h values at lower temperatures, ranging from 80 to 350 cm^{-1}. The h and k values of the present compositions, exhibiting fast diffusivity, are relatively low, showing that the flux of O^{2-} through the material is a surface exchange controlled process.

4 Conclusions

Summarising the suggestions arising from discussion of the results with respect to the effect of Sr and Ni doping in the perovskite-type oxides $La_{(1-x)}Sr_xCo_{(1-y)}Ni_yO_{3-\delta}$ on the electronic conductivity and oxygen transport, the following are concluded:

(a) The present oxides are excellent mixed conductors having high electronic conductivity in addition to the high oxygen transport rate.

(b) A strong interdependence between the Sr and Ni doping concentrations was found, in order achieve the maximum electronic conductivity. At each Sr substitution there is an optimum Ni content. The highest σ_e is presented by the composition containing 50 mol% Sr and 40 mol% Ni.

(c) The highest oxygen self-diffusion rate was found at 50 mol% Sr and 20 mol% Ni substitution for La and Co respectively.

(d) The oxygen flux process through the present oxides, exhibiting fast diffusivity, is strongly influenced by the surface exchange kinetics.

References

1. Ivers-Tiffee, E., Wersing, W., Schiessl, M. & Greiner, H., *Ber. Bunsenges, Phys. Chem.*, **94** (1990) 978.
2. Schiessl, M., Ivers-Tiffee, E. & Wersing, W., In *Proceedings of the 7th International Congress on High Technical Ceramics*, Montecatini terme, Italy, 24–30 June, 1990.
3. Palma, J. & Pascual, C., In *Proceedings of the 2nd International Symposium on SOFC*, ed. F. Grosz, P. Zegers, S. C. Singhal & O. Yamamoto. Commission of the European Communities, Brussels, 1991, EUR 13564 EN, p. 537.

4. Breiter, N. W., *Materials Science Forum*, **76** (1991) 245.
5. Rohland, B., *Materials Science Forum*, **76** (1991) 149.
6. Esaka, T. & Iwahara, H., *J. Appl. Electrochem.*, **15** (1985) 447.
7. Turrillas, X., Kilner, J. A., Kontoulis, I. & Steele, B. C. H., *J. Less Common Metals*, **151** (1989) 229.
8. Vischjager, D. J., Van Zoneren, A. A., Schoonman, J., Kontoulis, I. & Steele, B. C. H., *Solid State Ionics*, **40/41** (1990) 810.
9. Kontoulis, I. & Steele, B. C. H., *J. Mat. Sci. Eng. B*, (1992).
10. Cales, B. & Baumard, J. F., *J. Electrochem. Soc.*, **131** (1984) 2407.
11. Teraoka, Y., Zhang, H. M., Furukawa, S. & Yamazoe, N., *Chem. Lett.*, (1985) 1743.
12. Teraoka, Y., Nobunaga, T. & Yamazoe, N., *Chem. Lett.*, (1988) 503.
13. Teraoka, Y., Furukawa, S., Zhang, H. M. & Yamazoe, N., *Nippon Kagaku Kaishi*, (1988) 1084.
14. Iwahara, H., Esaka, T. & Mangahara, T., *J. Appl. Electrochem.*, **18** (1988) 173.
15. Steele, B. C. H., *Mater. Sci. Eng.*, **B13** (1992) 79.
16. Carter, S., Selcuk, A., Chater, R. J., Kajda, J., Kilner, J. A. & Steele, B. C. H., In *Proceedings of the 8th International Conference on Solid State Ionics*, Lake Louise, Alberta, Canada, 20–26 October, 1991, ed. P. S. Nicholson, M. S. Whittingham, G. Farrington, W. W. Smeltzer & J. Thomas, Amsterdam–London. Part 1, p. 597.
17. Teraoka, Y., Nobunaga, T., Okamoto, K., Miura, N. & Yamazoe, N., *Solid State Ionics*, **48** (1991) 207.
18. Yamamoto, O., Takeda, Y., Kanno, R. & Noda, M., *Solid State Ionics*, **22** (1987) 241.
19. Takeda, Y., Kanno, R., Noda, M., Tomida, Y. & Yamamoto, O., *J. Electrochem. Soc.*, **134** (1987) 2656.
20. Teraoka, Y., Yoshimatsu, M., Yamazoe, N. & Seiyama, T., *Chem. Lett.*, (1984) 893.
21. Zhang, H. M., Yamazoe, N. & Teraoka, Y., *J. Mater. Sci. Lett.*, **8** (1989) 995.
22. Teraoka, Y., Zhang, H. M., Okamoto, K. & Yamazoe, N., *Mat. Res. Bull.*, **23** (1988) 51.
23. Ftikos, Ch. & Steele, B. C. H., *J. Eur. Ceram. Soc.*, (1992).
24. Chater, R. J., Carter, S., Kilner, J. A. & Steele, B. C. H., In *Proceedings of the 8th* International Conference on Solid State Ionics, Lake Louise, Alberta, Canada, 20–26 October 1991, ed. P. S. Nicholson, M. S. Whittingham, G. Farrington, W. W. Smeltzer & J. Thomas, Amsterdam–London, p. 859.
25. Nakamura, T. & Choy, J. H., *J. Solid State Chem.*, **20** (1977) 233.
26. Jonker, G. H., *Philips Res. Rep.*, **24** (1969) 1.
27. Goodenough, J. B., Metallic oxides. In *Progress in Solid State Chemistry*, Vol. 6, ed. H. Reiss. Pergamon Press, Oxford–New York, 1971, p. 233.
28. Bhide, V. D., Rajoria, D. S., Rama Rao, G. & Rao, C. N. R., *Phys. Rev. B.*, **6** (1972) 1021.
29. Bhide, V. G., Rajoria, D. S., Rao, C. N. R., Rama Rao, G. & Jadhao, V. G., *Phys. Rev. B.*, **12** (1975) 2832.
30. Gopalakrishnan, J., Golsmann, G. & Reuter, B., *Z. Anorg. Allg. Chem.*, **424** (1976) 155.
31. Rao, C. N. R., Parkash, O. M., Bahadur, D., Ganguly, P. & Nagabhushana, S., *J. Solid State Chem.*, **22** (1977) 353.
32. Goodenough, J. B., *Mater. Res. Bull.*, **8** (1973) 423.
33. Gopalakrishnan, J., Golsmann, G. & Reuter, B., *J. Solid State Chem.*, **22** (1977) 145.
34. Kilner, J. A. & Brook, R. J., *Solid State Ionics*, **6** (1982) 253.
35. Steele, B. C. H., In *High Conductivity Ionic Conductors*, ed. T. Takahashi. World Scientific Publ., Singapore–New Jersey, 1989, p. 402.
36. Cook, R. L. & Sammelis, A. F., *Solid State Ionics*, **45** (1991) 311.